RSC Applied Polymers

ROYAL SOCIETY OF CHEMISTRY

PAPER

View Article Online
View Journal

Cite this: DOI: 10.1039/d5lp00281h

Effective and sustainable removal of a model fluorescent brightener using bicarbonate-loaded polyelectrolytes in a closed-loop CO_2 cycle

Eri Yoshida

Fluorescent brighteners (FBs), currently recognised as emerging contaminants, require effective removal from aquatic environments. However, no practical methods exist due to their high water solubility, the formation of toxic byproducts upon decomposition, and the lack of repeatable absorbent regeneration. This study demonstrates the efficient removal of a fluorescent brightener from water using cationic polyelectrolytes loaded with bicarbonates. Poly(allylammonium bicarbonate) (PAAm-BC), obtained from commercially available poly(allylamine) (PAA) by capturing carbonic acid, effectively removed disodium 4,4′-bis(2-sulfostyryl)biphenyl (DSBP) from water through ion exchange. The removal efficiency reached nearly 100%, independent of the molecular weight of PAAm-BC. The bicarbonate-loaded polymer incorporated DSBP as an electrostatic cross-linker; the incorporated DSBP aligned within the polymer composites, generating directional regions in their morphology. Under basic conditions (pH 12), the composites completely released DSBP, regenerating PAA, which reloaded bicarbonates upon CO_2 introduction and enabled subsequent removal. This reversible removal process, achieved through repeated basification and CO_2 introduction in a closed-loop CO_2 cycle, is potentially applicable to a wide range of anionic pollutants and offers a promising strategy for improving aquatic environments.

Received 9th September 2025,
Accepted 5th December 2025

DOI: 10.1039/d5lp00281h

rsc.li/rscapplpolym

Introduction

Anthropogenic contaminants have severely degraded the global environment through improper treatment and increasing emissions from households, facilities and industries. Emerging contaminants include micro- and nanoplastics from waste plastics, per- and polyfluoroalkyl substances (PFAS), liquid crystal monomers, polycyclic aromatic hydrocarbons, polychlorinated biphenyls, radionuclides, toxic agrochemicals, synthetic pesticides and antibiotic resistance genes in modified bacteria.[1,2] These pollutants disperse into the atmosphere, infiltrate soil and run off into rivers and oceans,[3,4] where they undergo further degradation and solubilisation. Consequently, they cause serious diseases through contaminated food and water and *via* the food web, leading to biodiversity loss and ecosystem disruption.[5]

Fluorescent brighteners (FBs) have recently emerged as overlooked contaminants. Although their toxicity was noted decades ago, they long received little attention, as they were considered safe and unlikely to cause serious effects such as carcinogenicity, mutagenicity or teratogenicity.[6–9] However, recent studies report that FBs can induce diseases, including gene mutations and eczema, and are now recognised as thyroid hormone-disrupting chemicals.[10,11] Among them, disodium 4,4′-bis(2-sulfostyryl)biphenyl (DSBP) is the most widely used FB and serves as a benchmark for assessing FB pollution in aquatic environments. DSBP exhibits higher toxicity than synthetic surfactants such as alkyl- and alkylbenzene sulfonates (ABSs), and even greater toxicity than PFAS, due to its strong binding affinity for human transthyretin, where it acts as a thyroid hormone ligand through its two sulfonate groups.[10] DSBP has also been shown to interact with the estrogen receptor[12] and with human serum albumin (HSA).[13] Given that HSA is the most abundant carrier protein in the circulatory system and delivers substances to diverse organs, the high DSBP–HSA affinity poses significant risks to multiple organ systems.[14,15]

DSBP is a common additive in industrial and household products, including detergents, dyes, fibres, plastics, papers, cosmetics and food,[3,16–23] as well as in medical and agricultural applications.[24,25] Its high structural stability and poor biodegradability[6,26–28] promote bioaccumulation, while its high solubility in water (17.6 g L^{-1} at 20 °C) makes its removal from aquatic environments difficult. Several approaches have been attempted for DSBP removal, including chemical methods such as detoxification by photodegradation,[17,28–30] oxidation with hypochlorite[31] and complexation with viologen.[32] However, these approaches can generate secondary pol-

Department of Applied Chemistry and Life Science, Toyohashi University of Technology, 1-1 Hibarigaoka, Tempaku-cho, Toyohashi 441-8580, Japan. E-mail: yoshida.eri.gu@tut.jp

lutants from decomposition products. Physical methods, including adsorption with activated carbon and solid-phase extraction, have proven effective for DSBP capture,[33,34] while methods used for the removal of other FBs and ABSs, such as cloud point extraction, membrane filtration and electrocoagulation,[35–37] could potentially be applied to DSBP. Nonetheless, these physical methods also present challenges, including the management of accumulated DSBP and adsorbent regeneration. To date, no sustainable method has been established for effective DSBP removal.

Poly(allylamine) (PAA) is commercially available and easily modified, enabling its broad design and conversion into unique materials,[38] including polymer surfactants[39] and biocompatible polymers for medical applications.[40] In recent years, PAA has also been reported as an effective CO_2 absorbent.[41] With its high CO_2 capacity, thermal stability, resistance to oxidative degradation, durability under high-pressure gas streams and low regeneration energy,[42–46] PAA can facilitate industrial utilisation of CO_2, thereby contributing to global warming mitigation. In aqueous solution, PAA captures CO_2 as carbonic acid, converting into poly(allylammonium bicarbonate) (PAAm-BC). PAAm-BC has been examined in terms of its thermal stability, durability under a nitrogen flow, regenerability for recycling, and performance as a polyelectrolyte.[41] This bicarbonate-loaded cationic polyelectrolyte further undergoes ion exchange with sulfate-based substances such as sodium dodecyl sulfate,[41] forming micro- and nanoarchitectures that incorporate the sulfate while releasing bicarbonates. With the aim of developing a sustainable strategy for DSBP removal from wastewater, this study demonstrates, for the first time, that PAAm-BC effectively captures DSBP through ion exchange and that the resulting polymer composites reversibly release DSBP, regenerating PAA under basic conditions without byproduct formation. The regenerated PAA subsequently reloads bicarbonates upon CO_2 introduction, thus establishing a closed-loop CO_2 cycle (Fig. 1). This approach is broadly applicable to other sulfonate-based fluorescent brighteners, highlighting its potential as a versatile platform for mitigating sulfonate pollutant contamination.

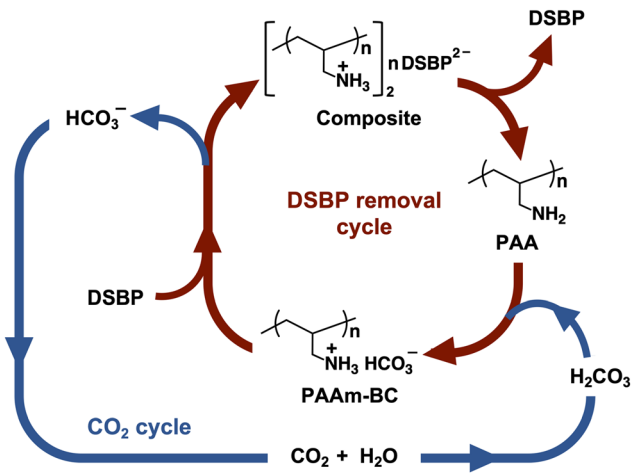

Fig. 1 Schematic illustration of DSBP removal by PAAm-BC in a closed-loop CO_2 cycle.

Experimental

Materials

PAA samples were kindly supplied by Nittobo Co., Ltd as 15 wt% aqueous solutions with weight-average molecular weights (M_w) of 1600 (*L*-PAA) and 15 000 (*H*-PAA) and as a 20 wt% solution with M_w of 5000 (*M*-PAA). Disodium 4,4′-bis(2-sulfostyryl)biphenyl (DSBP), purchased from Tokyo Chemical Industry, was used as received. Sodium hydroxide was purchased from FUJIFILM Wako Pure Chemical Corporation. Ultrapure water was obtained from a Merck Milli-Q® Integral MT-5 purification system. Carbon dioxide with >99.995% purity (vol%) was purchased from Taiyo Nippon Sanso Corporation.

Instrumentation

Light scattering measurements were performed at an angle of θ = 90° at 25 °C using a Photal Otsuka Electronics ELS-8000 electrophoretic light scattering spectrophotometer equipped with a system controller, an ELS controller and a He–Ne laser operating at λ = 632.8 nm. The hydrodynamic diameter (D_h) was determined by cumulant analysis, and the weight conversion distributions of D_h were obtained using Marquardt analysis.[47] UV spectra were recorded at 25 °C with a Shimadzu UV-160A UV–Vis spectrophotometer equipped with an Eyela NCB-1200 temperature circulator. Thermogravimetric analysis (TGA) was performed at a heating rate of 10 °C min^{-1} using a Hitachi High-Tech TG/DTA7200 under a nitrogen flow of 200 mL min^{-1}. Differential scanning calorimetry (DSC) was conducted at a heating rate of 20 °C min^{-1} with a Shimadzu DSC-60 instrument equipped with a TA-60WS system controller and an FC-60 nitrogen flow controller. Field-emission scanning electron microscopy (FE-SEM) observations were carried out using a Hitachi SU8000 at 0.7 kV without coating. The pH was measured with a Hanna Instruments HI991002N portable pH/ORP/°C meter.

Light scattering measurements and UV analysis

Ultrapure water (77.7 mL) was added to PAA (105.6 mg of a 15 wt% solution, corresponding to 15.84 mg (0.277 mmol) of the allylamine unit (AA) and 89.76 mg of water), resulting in an initial AA concentration of $[AA]_0 = 3.57 \times 10^{-3}$ mol L^{-1}. CO_2 was introduced by bubbling at a flow rate of 300 mL min^{-1} for 30 min, controlled with a flow meter, into the solution in a 200 mL round-bottom flask placed in a water bath at 25 °C under stirring. Aliquots (10 mL containing 0.0357 mmol of the allylammonium bicarbonate unit (AAm-BC)) of the resulting PAAm-BC solution were transferred into 20 mL sample bottles under continuous CO_2 flow. DSBP (100.5 mg, 0.179 mmol) was dissolved in water (5 mL), yielding an initial concentration of $[DSBP]_0 = 0.0357$ mol L^{-1}. The DSBP solution (0.1 mL contain-

ing 3.57×10^{-3} mmol) was added to the PAAm-BC solution (10 mL containing 0.0357 mmol of AAm-BC) at 25 °C with stirring. The mixture was stirred for 3 min at 25 °C, then allowed to stand at this temperature for 10 min without stirring, and subsequently subjected to light scattering to measure scattering intensity and hydrodynamic size, as well as UV analysis to determine transmittance.

FE-SEM observations

Precipitates were obtained by adding DSBP (80.2 mg, 0.143 mmol) dissolved in water (4 mL) to a PAAm-BC solution prepared from PAA (106.2 mg of a 15 wt% solution, corresponding to 15.93 mg (0.279 mmol) of AA) in water (78 mL) through CO_2 introduction. The precipitates were isolated by suction filtration and dried under vacuum for 3 h. The resulting yellow polymer composite powder was then subjected to FE-SEM measurements at 0.7 kV without coating.

Removal of DSBP

Water (77.0 mL) was added to PAA (105.1 mg of a 15 wt% solution, corresponding to 15.77 mg (0.276 mmol) of AA and 89.3 mg of water), resulting in $[AA]_0 = 3.58 \times 10^{-3}$ mol L^{-1}. CO_2 was introduced into the solution at 25 °C with stirring by bubbling at a flow rate of 300 mL min^{-1} for 30 min to obtain a PAAm-BC solution. DSBP (79.0 mg, 0.140 mmol) dissolved in water (4 mL) was then added dropwise to the PAAm-BC solution over 8 min at 25 °C under stirring, followed by an additional 2 min of stirring at the same temperature. Sodium hydroxide (1.1094 g, 27.735 mmol) was dissolved in water (10.05 mL). At 25 °C with stirring, aliquots (0.2 mL, containing 0.552 mmol) of the NaOH solution were added sequentially to the polymer composite solution containing the precipitates until complete release of DSBP was confirmed by UV absorbance. After each 0.2 mL addition, the mixture was subjected to pH measurement and UV analysis, in which a 0.1 mL aliquot of the mixture was diluted with water (10 mL) for DSBP absorbance determination.

Results and discussion

The capture of DSBP by PAAm-BC through ion exchange was investigated by stirring the mixture in water at 25 °C for 10 min. UV analysis demonstrated that DSBP was effectively captured, serving as an electrostatic cross-linker of PAAm-BC (Fig. 2), and that this cross-linking induced aggregation of the polymer composites. Fig. 3 shows the UV spectra of the mixtures of DSBP with PAAm-BC or PAA at a DSBP molar ratio of 0.5 to the allylammonium unit (DSBP/AAm) or the allylamine unit (DSBP/AA). The DSBP–PAA mixture exhibited characteristic absorption originating from DSBP, although the absorbance decreased by approximately 25% because the strong CO_2-absorbent PAA slightly captured CO_2 from the air during handling. In contrast, the mixture with PAAm-BC showed no absorption, owing to cross-linkable ion exchange with DSBP, which resulted in incorporation of DSBP into the precipitates of their insoluble composites (Fig. S1).

Fig. 4A shows the variations in transmittance, scattering intensity (SI) and hydrodynamic size (D_h) of PAAm-BC as a function of the DSBP/AAm ratio when DSBP was added to the PAAm-BC solutions derived from *L*-PAA, *M*-PAA and *H*-PAA

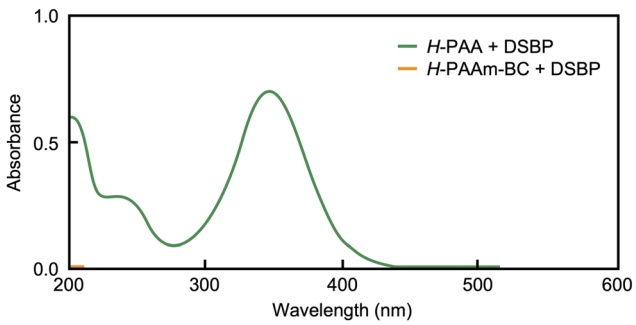

Fig. 3 UV spectra of the DSBP–PAA and DSBP–PAAm-BC mixtures. DSBP/AAm = DSBP/AA = 0.5. $[AA]_0 = [AAm\text{-}BC]_0 = 3.57 \times 10^{-3}$ mol L^{-1}.

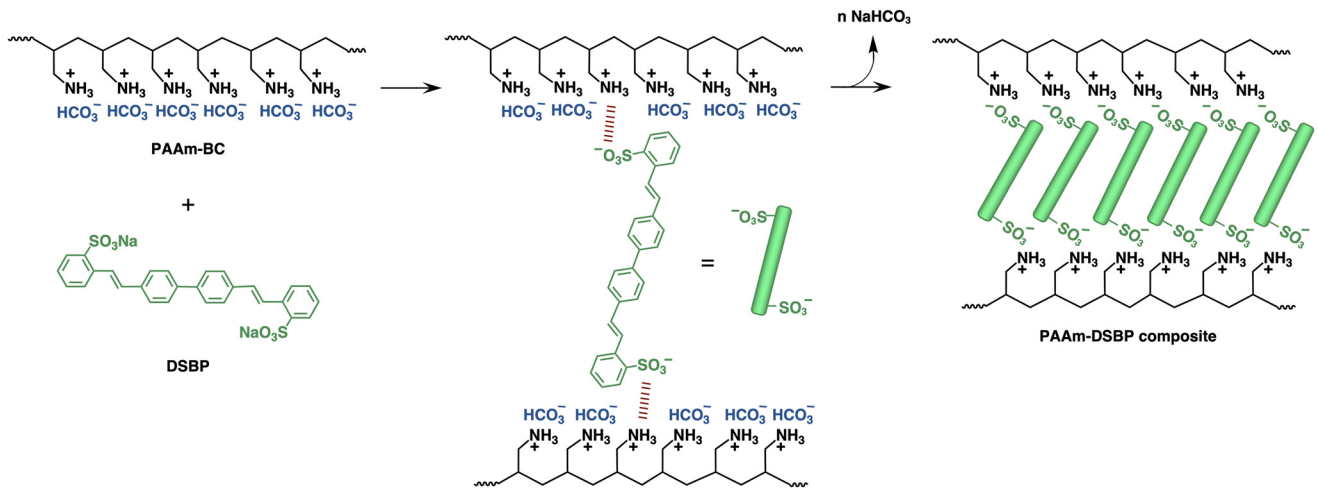

Fig. 2 Capture of DSBP by the bicarbonate-loaded polyelectrolytes through ion exchange.

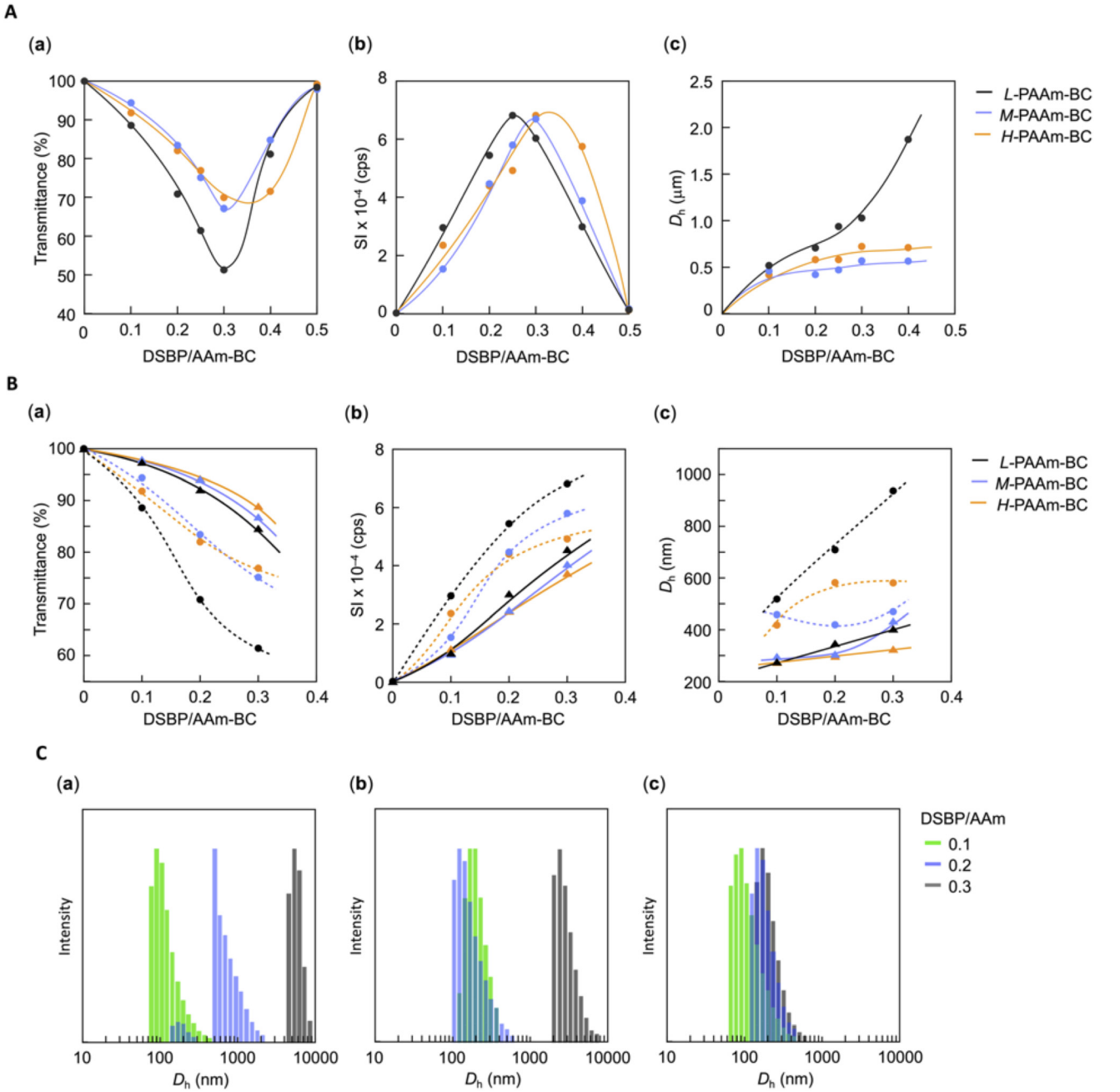

Fig. 4 (A) Variations in (a) transmittance, (b) scattering intensity and (c) hydrodynamic diameter of DSBP-captured PAAm-BC as a function of the DSBP/AAm-BC ratio. $[AAm\text{-}BC]_0 = 3.57 \times 10^{-3}$ mol L^{-1}. (B) Variations in (a) transmittance, (b) scattering intensity and (c) hydrodynamic diameter of DSBP-captured PAAm-BC as a function of the DSBP/AAm-BC ratio. $[AAm\text{-}BC]_0 = 3.57 \times 10^{-3}$ mol L^{-1} (dashed line) and 1.78×10^{-3} mol L^{-1} (solid line). (C) Weight conversion distributions in light scattering for (a) *L*-PAAm-BC, (b) *M*-PAAm-BC and (c) *H*-PAAm-BC at DSBP/AAm = 0.1, 0.2 and 0.3. $[AAm\text{-}BC]_0 = 1.78 \times 10^{-3}$ mol L^{-1}.

(denoted *L*-PAAm-BC, *M*-PAAm-BC and *H*-PAAm-BC, respectively). Upon addition of DSBP, the transmittance decreased more readily and to a greater extent for the shorter PAAm-BC, suggesting that the shorter PAAm-BC chains aggregate more easily through the ion exchange with DSBP. The transmittance decreased continuously up to a DSBP/AAm ratio of 0.30–0.35 and then increased beyond this ratio due to precipitation of the insoluble aggregates. At a ratio of 0.5, the transmittance was fully restored owing to the complete precipitation of the aggregates. Consistent with the transmittance changes, the SI exhibited maxima around a DSBP/AAm ratio of approximately 0.3. The maximum shifted to a lower ratio for the shorter PAAm-BC, indicating that the shorter chains facilitated aggregation. The D_h results revealed that *L*-PAAm-BC formed signifi-

cantly larger aggregates than *M*-PAAm-BC and *H*-PAAm-BC, suggesting that *L*-PAAm-BC tended to aggregate intermolecularly, whereas *M*-PAAm-BC and *H*-PAAm-BC primarily promoted intramolecular association.

PAAm-BC potentially facilitates intramolecular association in dilute solution. The solutions of PAAm-BC up to a DSBP/AAm ratio of 0.3, in which no precipitates were observed, were investigated in detail to clarify the aggregation behavior. Fig. 4B shows the transmittance, SI and D_h for the solutions at half the concentration of PAAm-BC. PAAm-BC showed only slight differences in transmittance and SI among the chain lengths, but a difference was discerned with increasing the DSBP/AAm ratio. In particular, *L*-PAAm-BC exhibited an increase in D_h as the DSBP ratio increased, whereas *H*-PAAm-BC showed a negligible change in D_h regardless of the DSBP ratio. In contrast, *M*-PAAm-BC initially showed D_h values comparable to those of *H*-PAAm-BC up to a DSBP ratio of 0.2; however, at a ratio of 0.3, the D_h of *M*-PAAm-BC approached that of *L*-PAAm-BC. This change implies that *M*-PAAm-BC undergoes a transition from intramolecular association to intermolecular aggregation.

The weight-conversion distribution analysis corroborated these aggregation behaviors (Fig. 4C). The distribution of *L*-PAAm-BC shifted markedly toward a higher D_h region as the DSBP ratio increased, whereas *H*-PAAm-BC exhibited only a slight shift at a ratio of 0.2 and no further shift at 0.3. In contrast, the distribution of *M*-PAAm-BC remained unchanged at a ratio of 0.2 but shifted toward a higher D_h region at 0.3. These observations indicate that the short PAAm-BC chains form insoluble complexes with DSBP, subsequently promoting intermolecular aggregation, whereas the long chains undergo intramolecular cross-linking *via* DSBP and remain as single-molecular aggregates. PAAm-BC of the intermediate chain length initially undergoes intramolecular association, followed by a transition to intermolecular aggregation.

The aggregation behavior determined the aggregate size, which in turn governed the precipitation rate. This was visually confirmed from photographs of the solutions at different DSBP ratios (Fig. 5 and Fig. S2). UV analysis further revealed that all DSBP molecules were incorporated into the precipitates of the polymer composites, demonstrating complete removal of DSBP from the aqueous solution (Fig. 6). The removal efficiencies of DSBP were nearly 100%, regardless of the molecular weight of PAAm-BC.

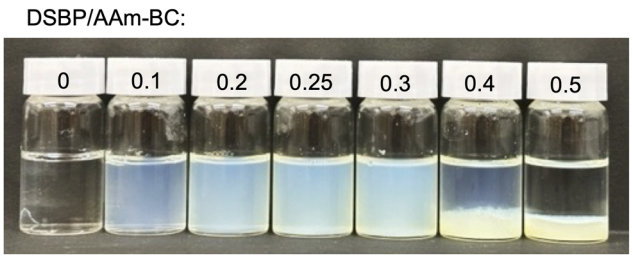

Fig. 5 A photograph of *L*-PAAm-BC solutions at different DSBP ratios.

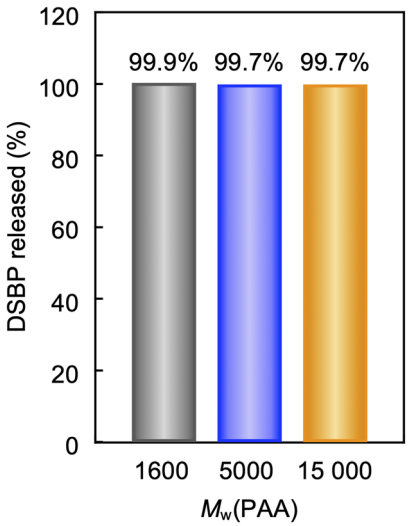

Fig. 6 Removal efficiencies of DSBP for PAA with different molecular weights. DSBP/AAm = 0.5.

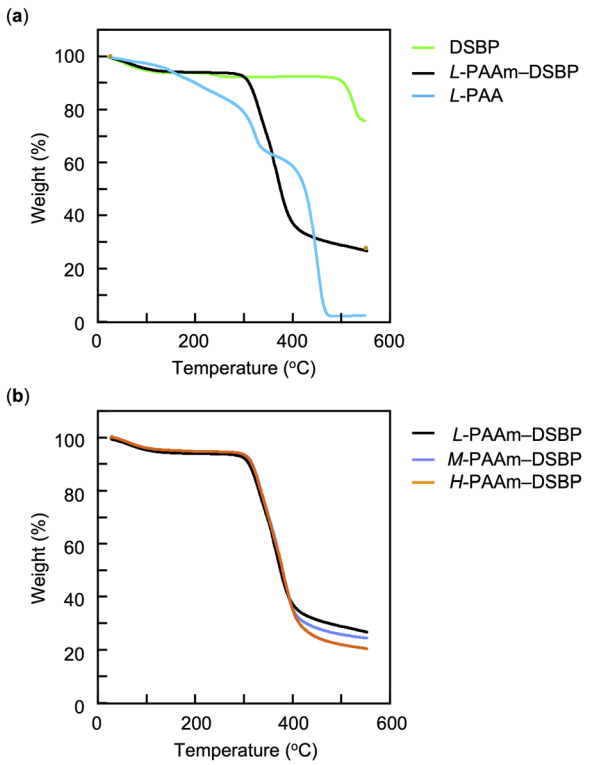

Fig. 7 TGA curves of (a) *L*-PAAm–DSBP composites (DSBP/AAm-BC = 0.5), *L*-PAA and DSBP and (b) *L*-PAAm–DSBP, *M*-PAAm–DSBP and *H*-PAAm–DSBP composites (DSBP/AAm = 0.5).

The composites with a DSBP/AAm ratio of 0.5 were isolated to evaluate thermal stability. Fig. 7 shows the TGA curves of the composites, together with those of PAA and DSBP. The composites displayed a sharp weight loss at 306.6 °C, independent of the molecular weight of PAAm-BC. This degradation corresponded to the first degradation step of PAA, observed at

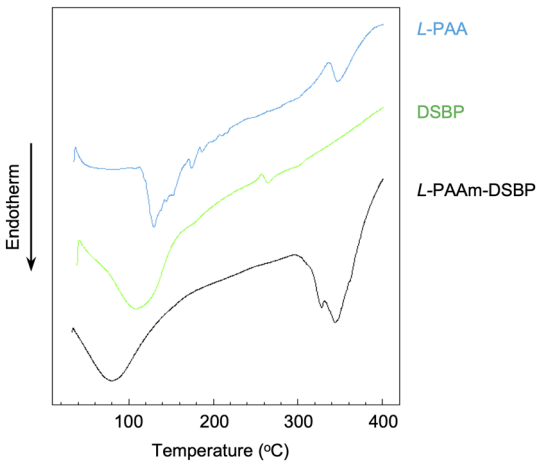

Fig. 8 DSC curves of *L*-PAAm–DSBP composites (DSBP/AAm-BC = 0.5), *L*-PAA and DSBP.

307.0 °C. Whereas PAA exhibited a second degradation at 422.2 °C, the composites showed no further weight loss and ultimately left a residue. This incomplete degradation resulted from the high thermal stability of DSBP, which decomposed only above 500 °C (Fig. S3).

DSC analysis revealed isotropic crystalline regions with disordered orientation in the composites (Fig. 8). These regions, originating from DSBP, extended from 40 to 150 °C with a peak maximum at 88.9 °C. The slightly lower melting point compared with pure DSBP suggested that the polymer chains in the composites hindered DSBP crystallisation. Melting of these regions was followed by that of the ammonium sulfonate moieties at 299.7 °C. This thermal behaviour was also unaffected by the molecular weight of PAAm-BC (Fig. S4).

The DSBP incorporated into the composites strongly influenced their morphology. While pure DSBP formed spherical particles with fine surface lines, the DSBP in the composites produced a cleavage-like morphology (Fig. 9). The linear and rigid DSBP molecules aligned within the composites through cross-linking of the polymer chains, creating directional regions in the composite structure. This morphological

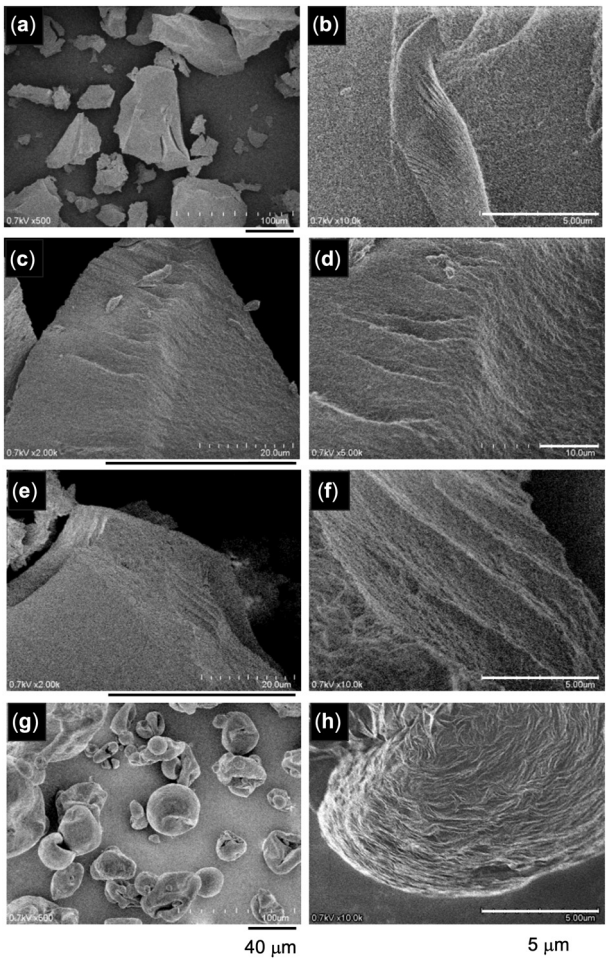

Fig. 9 FE-SEM images of (a and b) *L*-PAAm–DSBP composites, (c and d) *M*-PAAm–DSBP composites, (e and f) *H*-PAAm–DSBP composites and (g and h) DSBP. Black scale bars: 40 μm; white scale bars: 5 μm.

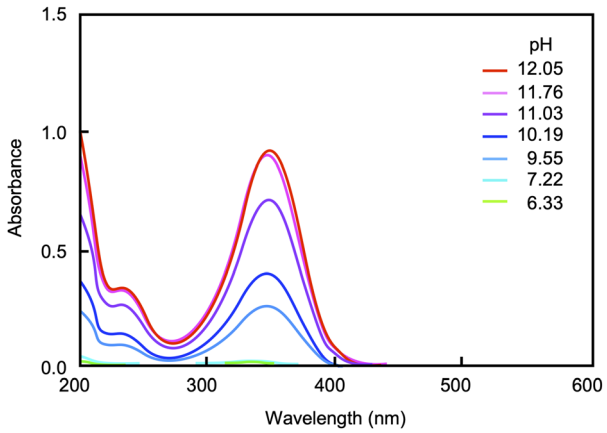

Fig. 10 UV absorbance of DSBP released from *L*-PAAm–DSBP composites at different pH values.

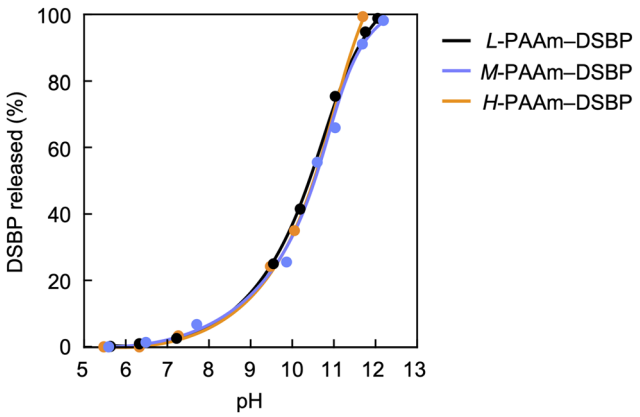

Fig. 11 Release efficiency of DSBP as a function of pH, determined from UV absorbance at λ = 348 nm.

change suggests that DSBP not only serves as a cross-linker but also directs the internal organisation of the polymer matrix.

The composites efficiently released the DSBP under basic conditions. As shown in Fig. 10, UV absorbance originating from DSBP increased with increasing pH, indicating release of DSBP molecules from the composites (Fig. S5). Plotting the absorbance at 348 nm *versus* pH confirmed complete release at approximately pH 12 (Fig. 11). Under such strongly basic conditions, the composites dissociated completely, releasing DSBP and regenerating deprotonated PAA (Fig. 12). This pH-dependent release of DSBP was independent of the molecular weight of PAAm-BC. Introduction of CO_2 into the basic solution reloaded bicarbonate

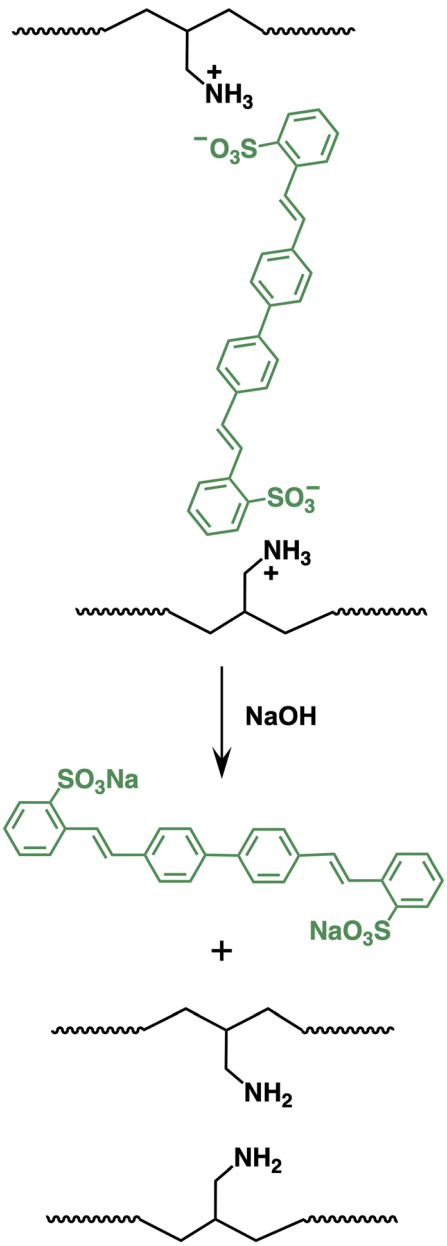

Fig. 12 Release of DSBP from the polymer composites under basic conditions.

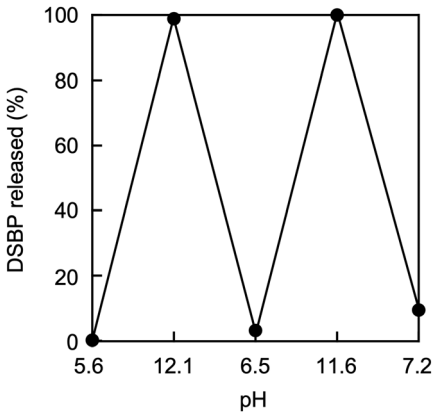

Fig. 13 Reversible capture and release of DSBP by *L*-PAAm-BC over repeated pH-change cycles, determined from UV absorbance at λ = 348 nm.

onto PAA, enabling recapture of DSBP. This capture and release of DSBP was completely reversible through repeated cycles of CO_2 introduction and basification, corresponding to loading and unloading of carbonic acid on PAA (Fig. 13 and Fig. S6). Thus, complete removal of this toxic additive by the bicarbonate-loaded absorbent, together with its full regeneration, was achieved in a sustainable closed-loop CO_2 cycle.

Conclusions

The bicarbonate-loaded polyelectrolyte, generated by capturing carbonic acid in water with a polymeric amine, effectively captured and removed the sulfonate-based fluorescent brightener from contaminated water through ion exchange. The bicarbonate-loaded polymer incorporated the toxic additive as an electrostatic cross-linker into the precipitates of its polymer composites. The low-molecular-weight polymer more readily captured the additive through intermolecular aggregation, whereas the high-molecular-weight polymer favoured intramolecular association. The medium-molecular-weight polymer underwent intramolecular association at low additive ratios and transitioned to intermolecular aggregation at higher ratios. The polymer composites released the fluorescent brightener completely under basic conditions, dissociating and reverting to the original polymeric amine. Upon CO_2 introduction, the polymeric amine reloaded bicarbonate and recaptured the pollutant. This reversible capture–release cycle enabled full regeneration of the absorbent through repeated CO_2 introduction and basification. The process relies on loading and unloading bicarbonate ions from the absorbent, establishing a sustainable closed-loop CO_2 cycle. This method for removing fluorescent brighteners is broadly applicable to a wide range of anionic pollutants, including sulfonate-based surfactants and dyes, per- and polyfluoroalkyl sulfonates and other toxic chemicals from diverse industrial fields such as medical care, food processing and dyeing, offering a promising approach to global environmental preservation.

Conflicts of interest

There are no conflicts to declare.

Data availability

All data supporting this study are available in the supplementary information (SI). Supplementary information is available. See DOI: https://doi.org/10.1039/d5lp00281h.

Acknowledgements

The author gratefully acknowledges Dr Mitsuo Oda of the Material Technology Department, Nagoya Municipal Industrial Research Institute, for conducting the TGA measurements, and this study was supported by the Japan Society for the Ppromotion of Science (JSPS) Grant-in-Aid for Scientific Research (Grant Number 23K04533).

References

1 F. Wang, L. Xiang, K. S.-Y. Leung, M. Elsner, Y. Zhang, Y. Guo, B. Pan, H. Sun, T. An, G. Ying, B. W. Brooks, D. Hou, D. E. Helbling, J. Sun, H. Qiu, T. M. Vogel, W. Zhang, Y. Gao, M. J. Simpson, Y. Luo, S. X. Chang, G. Su, B. M. Wong, T.-M. Fu, D. Zhu, K. J. Jobst, C. Ge, F. Coulon, J. D. Harindintwali, X. Zeng, H. Wang, Y. Fu, Z. Wei, R. Lohmann, C. Chen, Y. Song, C. S. Cid, Y. Wang, A. El-Naggar, Y. Yao, Y. Huang, J. C.-F. Law, C. Gu, H. Shen, Y. Gao, C. Qin, H. Li, T. Zhang, N. Corcoll, M. Liu, D. S. Alessi, H. Li, K. K. Brandt, Y. Pico, C. Gu, J. Guo, J. Su, P. Corvini, M. Ye, T. Rocha-Santos, H. He, Y. Yang, M. Tong, W. Zhang, F. Suanon, F. Brahushi, Z. Wang, S. A. Hashsham, M. Virta, Q. Yuan, G. Jiang, L. A. Tremblay, Q. Bu, J. Wu, W. Peijnenburg, E. Topp, X. Cao, X. Jiang, M. Zheng, T. Zhang, Y. Luo, L. Zhu, X. Li, D. Barceló, J. Chen, B. Xing, W. Amelung, Z. Cai, R. Naidu, Q. Shen, J. Pawliszyn, Y. Zhu, A. Schaeffer, M. C. Rillig, F. Wu, G. Yu and J. M. Tiedje, *Innovation*, 2024, **5**, 100612.
2 R. Naidu, B. Biswas, I. R. Willett, J. Cribb, B. K. Singh, C. P. Nathanail, F. Coulon, K. T. Semple, K. C. Jones, A. Barclay and R. J. Aitken, *Environ. Int.*, 2021, **156**, 106616.
3 N. M. Niloy, M. M. Haque and S. M. Tareq, *Environ. Nanotechnol., Monit. Manage.*, 2021, **15**, 100419.
4 M. Muschket, I. J. Neuwald, D. Zahn, A. H. Seelig, K. Jochen, T. P. Knepper and T. Reemtsma, *Water Res.*, 2024, **266**, 122436.
5 X. Li, X. Shen, W. Jiang, Y. Xi and S. Li, *Ecotoxicol. Environ. Saf.*, 2024, **278**, 116420.
6 J. B. Kramer, Fluorescent whitening agents, in *The Handbook of Environmental Chemistry: Detergents Volume 3F*, ed. N. T. de Oude, Springer-Verlag, New York, 1992, p. 351.
7 M. K. Keplinger, O. E. Fancher, F. L. Lyman and J. C. Calandra, *Toxicol. Appl. Pharmacol.*, 1974, **27**, 494–506.
8 A. W. Burg, M. W. Rohovsky and C. J. Kensler, *CRC Crit. Rev. Environ. Control*, 1977, **7**, 91–120.
9 C. Gloxhuber and H. Bloching, *Clin. Toxicol.*, 1978, **13**, 171–203.
10 Y. Gong, J. Sun, X. Wang, H. Barrett and H. Peng, *Environ. Sci. Technol.*, 2024, **58**, 10227–10239.
11 Y. Gong, D. Yang, J. Liu, H. Barrett, J. Sun and H. Peng, *Environ. Sci. Technol.*, 2023, **57**, 11913–11925.
12 D. B. D. Simmons, V. L. Trudeau, V. L. Marlatt, T. W. Moon, J. P. Sherry and C. D. Metcalfe, *Environ. Toxicol. Chem.*, 2008, **27**, 442–445.
13 L. Zhao, J. Liu, R. Guo, Q. Sun, H. Yang and H. Li, *RSC Adv.*, 2017, **7**, 27796–27806.
14 C. D. Kanakis, P. A. Tarantilis, M. G. Polissiou, S. Diamantoglou and H. A. Tajmir-Riahi, *J. Mol. Struct.*, 2006, **798**, 69–74.
15 A. Varshney, P. Sen, E. Ahmad, M. Rehan, N. Subbarao and R. H. Khan, *Chirality*, 2010, **22**, 77–87.
16 J.-M. A. Stoll and W. Giger, *Water Res.*, 1998, **32**, 2041–2050.
17 R. Gade, J. Ahemed, K. L. Yanapu, S. Y. Abate, Y.-T. Tao and S. Pola, *J. Environ. Chem. Eng.*, 2018, **6**, 4504–4513.
18 K. J. Smit and K. P. Ghiccino, *J. Polym. Sci., Part B: Polym. Phys.*, 1991, **29**, 1397–1405.
19 Q. Zhao, J. Sun, B. Liu and J. He, *Cellulose*, 2014, **21**, 2937–2950.
20 S. Toffanin, S. Kim, S. Cavallini, M. Natali, V. Benfenati, J. J. Amsden, D. L. Kaplan, R. Zamboni, M. Muccini and F. G. Omenetto, *Appl. Phys. Lett.*, 2012, **101**, 091110.
21 E. T. Iamazaki and T. D. Z. Atvars, *Langmuir*, 2007, **23**, 12886–12892.
22 Z. Zhong, W. Chen and J. Deng, *Microchem. J.*, 2024, **200**, 110409.
23 K. Y. Ko, C. A. Lee, J. C. Choi and M. Kim, *Food Addit. Contam.,: Part A*, 2014, **31**, 1451–1459.
24 A. Abbasi, M. Eslamian, D. Heyd and D. Rousseau, *Pharm. Dev. Technol.*, 2008, **13**, 549–557.
25 S. Xu, X. Wang, Y. Zhong, Y. Jin and J. Song, *ACS Agric. Sci. Technol.*, 2023, **3**, 996–1003.
26 F. Li, C. Wang, P. Jin, Y. Lin, Y. Zheng and J. Fan, *Chem. Eng. J.*, 2025, **517**, 164512.
27 T. Poiger, J. A. Field, T. M. Field, H. Siegrist and W. Giger, *Water Res.*, 1998, **32**, 1939–1947.
28 J. B. Kramer, S. Canonica, J. Hoigne and J. Kaschig, *Environ. Sci. Technol.*, 1996, **30**, 2227–2234.
29 P. Wong-Wah-Chung, G. Mailhot, J.-P. Aguer and M. Bolte, *Chemosphere*, 2006, **65**, 2185–2192.
30 J. M. Kesselman-Truttmann and S. J. Hug, *Environ. Sci. Technol.*, 1999, **33**, 3171–3176.
31 M. Blanco, L. Jiménez and I. Valverde, *Environ. Toxicol. Chem.*, 2001, **20**, 2193–2197.
32 E. J. Armstrong, H. Galas, R. S. Wylie, S. Zohrehvand, J. van Stam and C. H. Evans, *Can. J. Chem.*, 2021, **99**, 563–569.
33 M. R. Silva, M. A. Z. Coelho and M. C. Cammarota, *J. Hazard. Mater.*, 2008, **150**, 438–445.
34 H.-C. Chen and W.-H. Ding, *J. Chromatogr. A*, 2006, **1108**, 202–207.

35 M. Mustafa, E. I. Epelle, A. Macfarlane, M. Cusack, A. Burnsc and M. Yaseen, *RSC Adv.*, 2025, **15**, 12125–12151.
36 J. Han, X. Tang, Y. Wang, J. Li, L. Ni and L. Wang, *Water Environ. Res.*, 2017, **89**, 281–287.
37 I. Casero, D. Sicilia, S. Rubio and D. Pérez-Bendito, *Anal. Chem.*, 1999, **71**, 4519–4526.
38 A. Koutsianos, L. B. Hamdy, C. Yoo, J. J. Lee, M. Taddei, J. M. Urban-Klaehn, J. Dryzek, C. W. Jones, A. R. Barron and E. Andreoli, *J. Mater. Chem. A*, 2021, **9**, 10827–10837.
39 E. Yoshida, *Colloid Polym. Sci.*, 2010, **288**, 1321–1325.
40 E. Apuzzo, M. Agazzi, S. E. Herrera, A. Picco, G. Rizzo, C. Chavero, D. Bianchi, P. Smaldini, M. L. Cortez, W. A. Marmisolle, G. Padula, A. Seoane, M. L. Alomar, M. P. Denofrio, G. Docena and O. Azzaroni, *ACS Appl. Bio Mater.*, 2023, **6**, 4714–4727.
41 E. Yoshida, *RSC Sustainability*, 2024, **2**, 1837–1848.
42 J. Kothandaraman, A. Goeppert, M. Czaun, G. A. Olah and G. K. S. Prakash, *Green Chem.*, 2016, **18**, 5831–5838.
43 A. A. Olajire, *Energy*, 2010, **35**, 2610–2628.
44 J. Zhang, Y. Qiao, W. Wang, R. Misch, K. Hussain and D. W. Agar, *Energy Procedia*, 2013, **37**, 1254–1261.
45 T. N. Borhani and M. Wang, *Renewable Sustainable Energy Rev.*, 2019, **114**, 109299.
46 Y. Shen, C. Jiang, S. Zhang, J. Chen, L. Wang and J. Chen, *Appl. Energy*, 2018, **230**, 726–733.
47 D. W. Marquardt, *J. Soc. Ind. Appl. Math.*, 1963, **11**, 431–441.